Communication

Equilibrium/Nonequilibrium Initial Configurations in Forward/Reverse Electron Transfer within Mixed-Metal Hemoglobin Hybrids

Ami D. Patel, Judith M. Nocek, and Brian M. Hoffman

J. Am. Chem. Soc., **2005**, 127 (48), 16766-16767• DOI: 10.1021/ja0552242 • Publication Date (Web): 12 November 2005

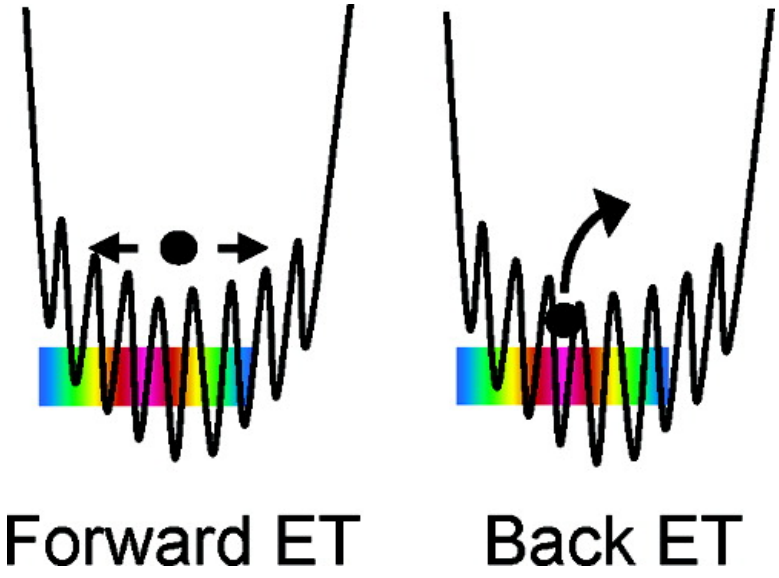

More About This Article

Additional resources and features associated with this article are available within the HTML version:

- Supporting Information
- Links to the 1 articles that cite this article, as of the time of this article download
- Access to high resolution figures
- Links to articles and content related to this article
- Copyright permission to reproduce figures and/or text from this article

View the Full Text HTML

J|A|C|S
COMMUNICATIONS

Published on Web 11/12/2005

Equilibrium/Nonequilibrium Initial Configurations in Forward/Reverse Electron Transfer within Mixed-Metal Hemoglobin Hybrids

Ami D. Patel, Judith M. Nocek, and Brian M. Hoffman*

Department of Chemistry, Northwestern University, 2145 North Sheridan Road, Evanston, Illinois 60208-3113

Received August 1, 2005; E-mail: bmh@northwestern.edu

Studies of long-range electron transfer (ET) within covalently linked systems typically seek an understanding of the ET process itself.[1,2] However, when the electron is transferred across a dynamic protein−protein interface, the observed kinetics frequently are controlled not by the ET process, but by the dynamics of protein recognition, binding, and conversion among an ensemble of bound configurations.[3−9] In general, such an interface will be characterized by a complicated energy landscape with multiple binding minima, with ET dominated by a subset of conformations in which the ET matrix element is largest; this is illustrated in the two-tier landscape of Figure 1.[10,11] This idea recently led us to recognize that the "forward" and "back" halves of a flash-induced protein−protein ET photocycle involve different initial configurational ensembles and, hence, should respond differently to the modulation of configuration interconversion dynamics.[5]

When the metalloporphyrin in a metal-substituted (M = Zn or Mg) hemoprotein is laser-flash excited to its lowest triplet state (^{3}D), this initiates ET from the triplet to a metal center in a bound acceptor protein (A), with rate constant, k_f, eq 1

$$[^3DA] \xrightarrow{k_f} [D^+A^-]\ (I) \qquad (1)$$

This forward ET reaction is initiated with the excited complex, [^{3}DA], in an equilibrium ensemble of configurations, the majority of which are likely to exhibit less than the maximal ET rate (Figure 1 bottom), and thus ET should be facilitated by conformational conversion to the more reactive configurations. In contrast, the charge-separated intermediate complex, **I**, is formed in the non-equilibrium set of configurations with maximal ET matrix elements, and it would be expected to return to the ground state with the largest possible rate constant, k_b, eq 2

$$\mathbf{I} \xrightarrow{k_b} [DA] \qquad (2)$$

unless conformational interconversion "breaks the connection" and the complex first converts to a less-reactive substate. With this analysis, the forward reaction should be slowed as dynamic processes are quenched by increases in viscosity (η); the back reaction should show a differential response to viscosity, with the extreme case being an *increasing* rate, if departure from the reactive configuration(s) is competitive with the ET event.[12] Thus viscosity variations of the photocycle offer a unique window into the interfacial dynamics of a protein−protein complex.

Mixed-metal hemoglobin (Hb) hybrids provide an ideal system with which to study ET between protein redox partners.[13,14] The tetramer does not dissociate into dimers under conditions employed here and can be treated as two independent, predocked [α_1 β_2] protein−protein ET complexes[13−16] (Chart 1). Thus they seemingly would be represented by a simple, tier 1, docking energy landscape (Figure 1, top). Recently, however, we reported that k_f and k_b for the [α_2(Zn), β_2(Fe^{3+}N$_3^-$)] hybrid at pH 8 showed differential

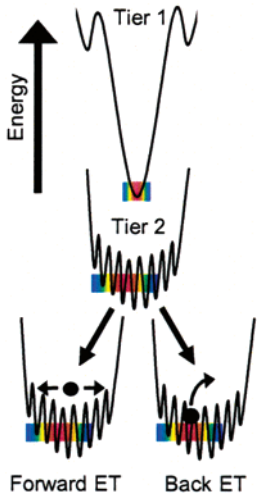

Figure 1. Proposed energy landscape for Hb hybrid ET complexes, with "rainbow" denoting ET-active configurations. The black dots (●) represent the system point: (*left*) for the equilibrium ensemble of configurations at the beginning of the photoinitiated ET process; (*right*) for the initial, nonequilibrium configuration in which the ET intermediate is formed. Arrows within the landscape indicate conformational interconversion.

Chart 1

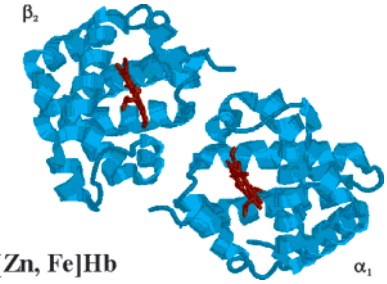

responses to increasing viscosity, suggestive that such a one-tier representation is not appropriate for ET within the hybrids and that ET may be influenced by conformational interconversion within second-tier substates on the energy landscape (Figure 1, bottom).[5] The forward rate constant, k_f, decreased with increasing η, as expected for ET photoinitiated within an equilibrium ensemble of interconverting configurations, but k_b showed little viscosity dependence. We now report that k_f and k_b for the hybrid at pH 7 show the extremes of behavior possible for a two-tier landscape: k_f decreases as η increases, while in sharp contrast, the rate constant, k_b, *increases* strongly with increasing η (Figure 2).

The ^{3}Zn porphyrin in an α chain of the [α(Zn),β(Fe^{2+})] hybrid decays exponentially, with an intrinsic decay rate constant, $k_D \sim 50\ s^{-1}$. In the [α(Zn),β(Fe^{3+}N$_3^-$)] hybrid, the ^{3}α(Zn) decay (rate constant k_{obs}) is enhanced through ET quenching (rate constant k_f) to form the charge-transfer intermediate, **I** (eq 1): $k_{obs} = k_f + k_D$.[5,15,17] The rate constant for the return of **I** to ground (eq 2, k_b) is

10.1021/ja0552242 CCC: $30.25

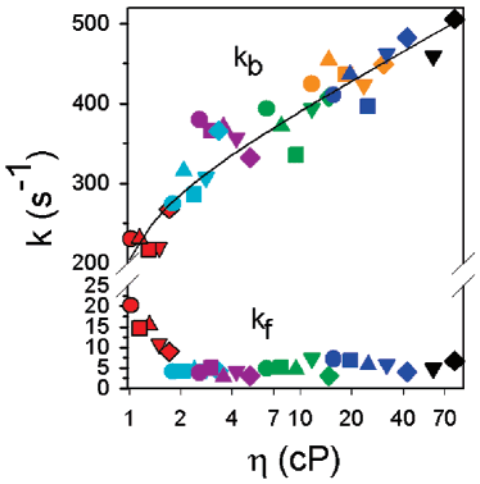

Figure 2. Viscosity dependence of k_b and k_f for the [α(Zn),β($Fe^{3+}N_3^-$)] hybrids at pH 7. Glycerol concentrations (w/w): red-0%, cyan-20%, purple-30%, green-50%, orange-60%, blue-65%. Sucrose concentrations (w/w): black-54%. Temperatures: (●) 20 °C; (■) 15 °C; (▲) 10 °C; (▼) 5 °C; (◆) 0 °C. Fitting time course of **I** gives k_{obs} and k_b; $k_f = k_{obs} - k_D$. Uncertainties: k_b, ±20 s^{-1}; k_f, ±5 s^{-1}. *Conditions*: 50 mM potassium phosphate, 100 mM NaN_3, 50 μM phytic acid (IHP), and 5 μM hybrid.

greater than k_{obs}, and as a result, **I** appears with rate constant k_b and decays with k_{obs}.[5] The two ET rate constants, k_f and k_b, were determined for the hybrid in solutions where η was increased to 42 cP by addition of glycerol and/or cooling; higher viscosities were achieved with cooled sucrose solutions (Figure 2).[18−20]

Earlier, we reported that for the [α(Zn),β($Fe^{3+}N_3^-$)] hybrid in pH 8 aqueous buffer $k_f = k_{obs} - k_D = 25\ s^{-1}$ ($T = 20$ °C),[5] and decreases with increasing glycerol concentration; for hybrids with other ligands (CN^- and H_2O), it decreases with cooling.[21,22] As seen in Figure 2, at pH 7, the small k_f for the [α(Zn),β($Fe^{3+}N_3^-$)] hybrid initially decreases with decreasing temperature/increasing viscogen/solution viscosity, then quickly levels off.

The ET return is much faster, $k_b = 230\ s^{-1}$ at $\eta = 1$ cP, $T = 20$ °C. In sharp contrast with k_f for the hybrid, and ET rates in general, k_b shows a strong *increase* with addition of glycerol or sucrose and with cooling, for example, doubling to $k_b = 470\ s^{-1}$ in 50% glycerol buffer at 0 °C. Figure 2 shows that the increase in k_b is well represented by a single, well-defined curve with increasing η, independent of temperature and viscogen. Previous studies of the temperature dependence of k_b for hybrid in buffered ethylene glycol solution[23] and in poly(vinyl alcohol) films with ligands other than azide[22] showed that k_b decreases upon cooling, indicating that the behavior in these solutions does not reflect an intrinsic temperature dependence of k_b; indeed, it appears that k_b for the [α(Zn),β($Fe^{3+}N_3^-$)] hybrid may decrease slightly upon cooling for some glycerol concentrations. Likewise, the increase in k_b with increasing glycerol does *not* appear to reflect increases in osmotic stress,[24] changes in water activity,[25] or specific interactions with increasing viscogen concentration. First, several pairs of solutions with different percentages of glycerol (osmotic pressure, water activity) and different temperatures, but the same η, show the same value of k_b. Second, when high η is achieved by addition of sucrose, the values of k_b (and k_f) follow the same η dependence (Figure 2). The only solution parameter that is seen to correlate well with k_b is η. While k_b strongly increases with η at pH 7, it is roughly independent of η at pH 8.[5] We surmise that the heightened response of k_b to increasing viscosity at pH 7 reflects alterations of the Hb dimer−dimer interface with pH.[26−29]

In summary, the behavior of the ET photocycle for the [α(Zn),β($Fe^{3+}N_3^-$)] hybrid in fact follows expectations for an ET photocycle within a complex represented by the two-tier energy landscape of Figure 1. Forward ET is initiated in an equilibrium ensemble of configurations, is assisted by conformational fluctuations into reactive configuration(s), and is impeded by restricting those fluctuations with increasing η. In contrast, the ET intermediate is formed in a nonequilibrium ensemble of reactive configurations, and back ET is facilitated when an increase in viscosity hinders competing conformational conversion to less-reactive configurations. Future experiments will extend this novel use of ET measurements to explore dynamics at a protein−protein interface.

Acknowledgment. This work was supported by the NIH (HL 62303) and benefited from discussions with Prof. Igor Kurnikov.

References

(1) Balzani, V. *Electron Transfer in Chemistry*; Wiley-VCH: Weinheim, New York, 2001.
(2) Marcus, R. A.; Sutin, N. *Biochim. Biophys. Acta* **1985**, *811*, 265−322.
(3) Nocek, J. M.; Zhou, J. S.; De Forest, S.; Priyadarshy, S.; Beratan, D. N.; Onuchic, J. N.; Hoffman, B. M. *Chem. Rev.* **1996**, *96*, 2459−2489.
(4) Liang, Z.-X.; Kurnikov, I. V.; Nocek, J. M.; Mauk, A. G.; Beratan, D. N.; Hoffman, B. M. *J. Am. Chem. Soc.* **2004**, *126*, 2785−2798.
(5) Hoffman, B. M.; Celis, L. M.; Cull, D. A.; Patel, A. D.; Seifert, J. L.; Wheeler, K. E.; Wang, J.; Yao, J.; Kurnikov, I. V.; Nocek, J. *Proc. Natl. Acad. Sci. U.S.A.* **2005**, *102*, 3564−3569.
(6) Ivkovic-Jensen, M. M.; Kostic, N. M. *Biochemistry* **1997**, *36*, 8135−8144.
(7) Feng, C.; Kedia, R. V.; Hazzard, J. T.; Hurley, J. K.; Tollin, G.; Enemark, J. H. *Biochemistry* **2002**, *41*, 5816−5821.
(8) Lasey, R. C.; Liu, L.; Zang, L.; Ogawa, M. Y. *Biochemistry* **2003**, *42*, 3904−3910.
(9) Schlarb-Ridley, B. G.; Mi, H.; Teale, W. D.; Meyer, V. S.; Howe, C. J.; Bendall, D. S. *Biochemistry* **2005**, *44*, 6232−6238.
(10) Despa, F.; Wales, D. J.; Berry, R. S. *J. Chem. Phys.* **2005**, *122*, 024103/1−024103/8.
(11) Frauenfelder, H.; Sligar, S. G.; Wolynes, P. G. *Science* **1991**, *254*, 1598−1603.
(12) Related observations have been made with an ET model. Shafirovich, V. Y.; Batova, E. E.; Levin, P. P. *J. Phys. Chem.* **1993**, *97*, 4877−4879.
(13) Natan, M. J.; Kuila, D.; Baxter, W. W.; King, B. C.; Hawkridge, F. M.; Hoffman, B. M. *J. Am. Chem. Soc.* **1990**, *112*, 4081−4082.
(14) Gingrich, D. J.; Nocek, J. M.; Natan, M. J.; Hoffman, B. M. *J. Am. Chem. Soc.* **1987**, *109*, 7533−7534.
(15) Kuila, D.; Natan, M. J.; Rogers, P.; Gingrich, D. J.; Baxter, W. W.; Arnone, A.; Hoffman, B. M. *J. Am. Chem. Soc.* **1991**, *113*, 6520−6526.
(16) Miyazaki, G.; Morimoto, H.; Yun, K.-M.; Park, S.-Y.; Nakagawa, A.; Minagawa, H.; Shibayama, N. *J. Mol. Biol.* **1999**, *292*, 1121−1136.
(17) Hybrids were prepared and kinetics measured as described in ref 5. Triplet decays were recorded at 475 nm, and signals for the ET intermediates were acquired at triplet isosbestic point, 436 nm.
(18) Jas, G. S.; Eaton, W. A.; Hofrichter, J. *J. Phys. Chem. B* **2001**, *105*, 261−272.
(19) Mathlouthi, M.; Reiser, P.; *Sucrose: Properties and Applications*, 1995.
(20) Miner, C. S.; Dalton, N. N. *Glycerol*; Reinhold Pub. Corp.: New York, 1953.
(21) Peterson-Kennedy, S. E.; McGourty, J. L.; Kalweit, J. A.; Hoffman, B. M. *J. Am. Chem. Soc.* **1986**, *108*, 1739−1746.
(22) Dick, L. A.; Malfant, I.; Kuila, D.; Nebolsky, S.; Nocek, J. M.; Hoffman, B. M.; Ratner, M. A. *J. Am. Chem. Soc.* **1998**, *120*, 11401−11407.
(23) Kuila, D.; Baxter, W. W.; Natan, M. J.; Hoffman, B. M. *J. Phys. Chem.* **1991**, *95*, 1−3.
(24) Goldbeck, R. A.; Paquette, S. J.; Kliger, D. S. *Biophys. J.* **2001**, *81*, 2919−2934.
(25) Parsegian, V. A.; Rand, R. P.; Rau, D. C. *Proc. Natl. Acad. Sci. U.S.A.* **2000**, *97*, 3987−3992.
(26) Huang, Y.; Yonetani, T.; Tsuneshige, A.; Hoffman, B. M.; Ackers, G. K. *Proc. Natl. Acad. Sci. U.S.A.* **1996**, *93*, 4425−4430.
(27) Daugherty, M. A.; Shea, M. A.; Ackers, G. K. *Biochemistry* **1994**, *33*, 10345−10357.
(28) Kavanaugh, J. S.; Rogers, P. H.; Arnone, A. *Biochemistry* **2005**, *44*, 6101−6121.
(29) Mueser, T. C.; Rogers, P. H.; Arnone, A. *Biochemistry* **2000**, *39*, 15353−15364.

JA0552242